Article Contr. Atmos. Phys., November 1999, p. 317–328
0005-8173/99/04 0317-12 $ 3.00/0 Vol. 72, No. 4 317

The Inland Penetration of Sea Breezes

A. B. C. TIJM[1], A. J. VAN DELDEN, AND A. A. M. HOLTSLAG[2]

Institute for Marine and Atmospheric research, Utrecht University (IMAU), Princetonplein 5, NL 3584 CC Utrecht, The Netherlands
[1] present affiliation: Royal Netherlands Meteorological Institute (KNMI), Postbus 201, NL 3730 AE De Bilt, The Netherlands
[2] present affiliation: Meteorology and Air Quality Section, Wageningen University, Wageningen, The Netherlands

(Manuscript received November 09, 1998; accepted March 17, 1999)

Abstract

The inland penetration of sea breezes is studied with observations and a two-dimensional mesoscale model. An anomalously high percentage of Northerly winds as compared to the average frequency distribution, is observed in the evening in the month of May, 1989, at a station about 100 km inland. In more than 50% of the sea-breeze cases during this very dry and sunny month, the wind shifted to this Northerly direction around 21 UTC. The model output of this month shows that this anomaly is caused by deep inland penetration of the sea breeze. From sensitivity experiments with the model it is derived that the inland penetration distance is determined mostly by the forcing through the differential heating and the magnitude of the opposing large-scale flow. With a linear combination of the scaled maximum sea-breeze strength and the opposing large-scale flow, the inland penetration of the sea breeze can be scaled.

1 Introduction

Sea breezes most often occur in the Netherlands during the spring and summer. This is the time when the North Sea is relatively cold and the sun reaches its minimum zenith angle. Therefore, the differential heating of the air over land and over sea can be large, and on clear days, with a weak large-scale flow, sea breezes develop. In the mid latitudes, these sea breezes usually travel from 5 to 50 km inland (Atkinson, 1981), sometimes even more. In a very extensive study of the inland penetration of sea breezes in southern England, Simpson et al. (1977) find that about 8% of the sea breezes that travel about 40 km inland also reach a station that lies about 100 km inland. If we take into account that only a part of all the sea breezes that develop near the coast travel 40 km inland, we must conclude that probably less than 5% of all sea breezes travel more than 100 km inland at latitudes of about 50°. So, very deep inland penetration of sea breezes (100 km or more) is possible, but seems rather unlikely.

Van Delden (1993) investigated the pressure perturbation distribution and the frequency distribution of the wind direction in the Netherlands during the month of May, 1989. As this month was one of the sunniest ever recorded in the Netherlands, a high number of sea breezes developed near the Dutch West-coast. The frequency distributions shown by Van Delden indicate that sea breezes occur near the Dutch West-coast on about 40% of the days during this month, where the onset of the sea breeze is defined as the moment that the wind becomes onshore due to a local circulation, induced by differential heating, while the large-scale wind is directed offshore. He also finds an unusual high frequency of Northerly winds during the evening at a station 100 km inland. This Northerly wind occurs on about 60% of the days with sea breezes. This is an order of magnitude higher than the frequency of very deep inland penetrating sea breezes (100 km or more) found for the United Kingdom by Simpson et al. (1977).

Together with the wind field anomaly, Van Delden finds an anomaly in the surface pressure field. The

combination of these two anomalies resembles a gravity-inertia wave, which travels inland at a speed of about 20 km h^{-1}. The gravity-inertia wave seems to originate near the West-coast, which leads to the conclusion that the initiation of this effect can be attributed to the developing sea breeze. It is known from theory and observations that the process of geostrophic adjustment can initiate these waves.

In this study we investigate the cause of the high frequency of Northerly winds far inland in the evening, that cannot be explained by a synoptic-scale pressure gradient, as it is not visible in the wind direction frequency distributions at other stations. This will be done by simulating the first 29 days of this month with the model that is described in Tijm et al. (1999). With these simulations we attempt to reproduce the observed frequency distributions of the wind direction at a few stations that lie at different distances from the coast, roughly on a line perpendicular to the coast.

In Section 2 we discuss the observations. The model and the initial conditions are discussed in Section 3. Section 4 is devoted to a discussion of the simulated frequency distributions of the wind direction. Section 5 contains results of a few sensitivity experiments concerning the inland penetration of the sea breeze. In Section 6 a scaling of these results is given. In Section 7 we study the daily cycle of the surface pressure perturbation to see if there is a connection between the daily pressure cycle and the maximum frequency of northerly winds in the evening far inland.

2 Observations

The stations concerned (330, 210, 260 and 375, see Figure 1 for the positions of the stations used) roughly lie along a line perpendicular to the coast that crosses the coast near station 210. The line is rotated 30° clockwise compared with a line going from West to East. This means that sea breezes at the western coast near station 210 blow from directions ranging from 220° to 20°. These stations are situated at the coast-line (station 330) up to 100 km inland (station 375). In the study of Van Delden (1993), one of the stations used is station 348. Although it lies almost on the imaginary line between stations 210 and 375, we will not use this station in this study because it shows a rather different wind-direction frequency distribution than expected that is probably caused by effects generated perpendicular to the imaginary line through the other stations. A possible explanation of the origin of this effect will be given in the discussion of the observations below. Station 554 is not used in the frequency distribution study because there is no data available on 10 of the 29 days in this period.

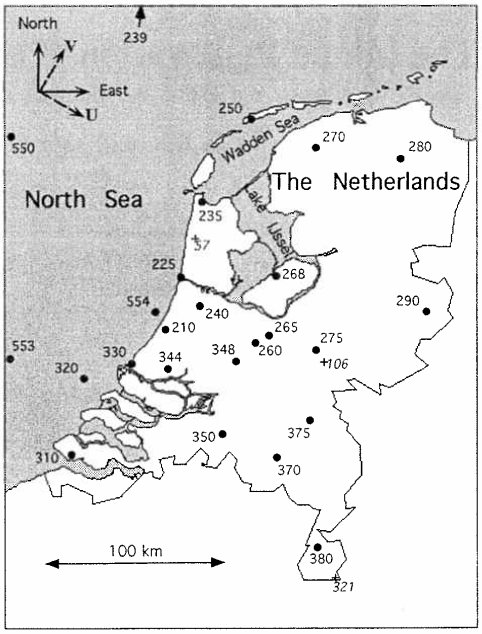

Figure 1: The Netherlands with the observation stations and some surface elevations in m (italic).

To calculate the frequency distributions of the wind direction, the wind direction is divided into 12 classes. Each class spans 30°, e.g. with the class of 180° spanning the range of 165° to 195°. A frequency of 38% from a certain direction means that the wind blew from that particular direction (±15°) during a given hour on 11 out of the 29 days (1–29 May, 1989) of this study.

With a monthly total sunshine of up to 341 hours at Vlissingen (station 310, see Figure 1), the daily average is 11 hours. The sea-surface temperature at station 553 is 8.5°C at the beginning of the month and increases to 12°C near the end of the month. With an average maximum air temperature over land of around 20°C and highest maximum temperatures around 30°C, the temperature difference between the air over sea and over land is large, especially during the afternoon, leading to many sea-breeze circulations during this month.

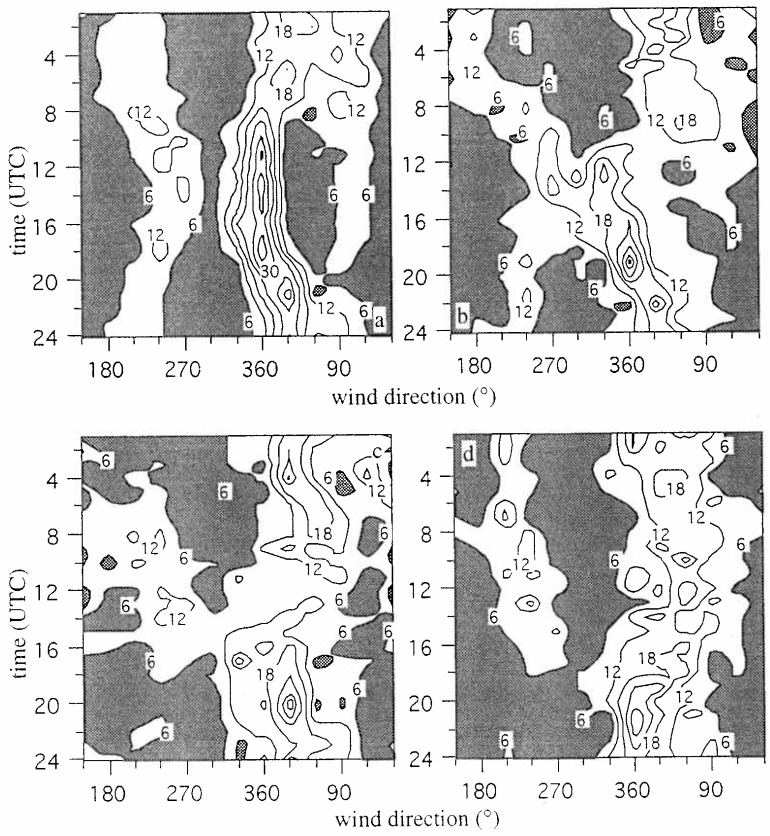

Figure 2: The observed frequency distributions (%) of the wind direction at stations 330 (a), 210 (b), 260 (c) and 375 (d) in the period from 1 to 29 May, 1989.

The 29-day average frequency distribution of the wind direction at station 330 clearly shows the influence of the sea breeze (see Figure 2a). During the evening and night the maximum frequency is found for a direction of 30° to 60°. During the night, the distribution is very broad with a frequency larger than 12% for directions ranging from 30° to 120°. During the day the frequency distribution narrows with the maximum frequency shifting to 0°, which means that the wind has a component blowing onshore, presumably caused by the sea breeze. The maximum shifts to a direction of 30° during the evening. A second maximum, that is much weaker than the strong maximum near 0°, is situated between 180° and 270°. This maximum also shows a small shift from 210° to 270° during the day. At this station there is no clear indication that the wind veers further to Northwest and North later in the afternoon and evening. The sea breezes, defined by a shift of the wind direction from offshore to onshore that is not caused by a synoptic-scale pressure system, set in at this station after 8 UTC.

Although station 210 lies only 3 km from the coastline, the frequency distribution (Figure 2b) differs strongly from that at station 330. The frequency distribution at station 210 shows a very pronounced daily cycle. Two maxima can be detected during the night. The strongest and broadest maximum occurs for directions around 60°, the weaker maximum is situated around 180°. After 11 UTC the sea breezes reach this station, causing the maxima to shift to 330° and 270° respectively. During the afternoon

the wind shifts further to the North. In the evening very high percentages of 42% for a direction of 0° at 19 UTC and 36% for a direction of 30° at 22 UTC are recorded.

At station 260 (see Figure 2c), the maximum frequency shifts from 30° to 60° early in the morning. Between 9 and 16 UTC, the frequency distribution does not show a pronounced maximum. At 17 UTC, a high frequency is found for a direction of 330°, which is presumably caused by the onset of sea breezes. This time of sea-breeze onset compares well with the average time of onset of deep-penetrating sea breezes in southern England (Simpson et al., 1977) that lies roughly at the same latitude as the Netherlands and has similar surface characteristics. After 17 UTC the maximum frequency quickly shifts to 30° (parallel to the West coast).

Far inland, at station 375, the wind direction also shows a maximum frequency at 30° to 60° during the night and early morning (see Figure 2d). The most striking feature is that the wind blows from a direction of 0° ±15° at 22 UTC on 11 of the 29 days (38%). A study of the individual days (not shown here) shows that on 4 of these days the Northerly flow around 21 UTC was not associated with the sea breeze, because the large-scale flow was Northerly at and preceding 21 UTC. On the other 7 days, sea breezes develop at the coast and a clear wind shift can be observed around 21 UTC. The total number of days with sea breezes in this period of 29 days was 12, so on about 60% of the days with sea breezes, the wind at station 375 was influenced in some way by these sea breezes.

The gravity-inertia waves in the explanation given by Van Delden should appear in the frequency distributions as high frequencies of Southerly winds that quickly shift to Northwest and North. Therefore, the high frequency of Northerly winds at station 375 should be preceded by a high frequency of Southerly winds with about the same magnitude. A detailed investigation of the individual days with a clear wind shift around 22 UTC shows that this behaviour of the wind direction cannot be found at station 375, resulting in some doubt about the gravity-inertia-wave-like structure of the phenomenon causing the high frequency of Northerly winds.

In the next sections of this study we try to answer the question: what causes this high frequency of Northerly winds far inland and is this caused by the sea breezes?

3 Model Setup and Parameters

To answer the above question we use a two-dimensional hydrostatic mesoscale model that is described in Tijm et al. (1999). Since the model is kept as simple as possible, it requires only limited computational resources, enabling us to study a long period and to investigate the impact of modifying important parameters. In the version of the model used here, the vertical turbulent momentum and heat fluxes are calculated with the diagnostic non-local scheme described in Holtslag and Boville (1993). The model has 71 grid points in the horizontal direction with a grid distance of 5 km. There are 40 grid points in the vertical direction with a grid-point distance that increases with increasing height. The model plane is projected along the observational transect and lies perpendicular to the West coast near station 210. As the Dutch West coast is nearly straight, we can use the two-dimensional model to study the sea breezes that develop near this western coast-line.

To simulate the frequency distribution of the wind direction and to find an explanation of the high frequencies of the Northerly wind direction found far inland, we perform 29 runs with the model corresponding to the first 29 days of May, 1989. The model runs start at 0 UTC and finish at 24 UTC. For every new day in the simulation sequence the entire model domain is initialized with new profiles for the wind and temperature, so we do not initialize the pressure distribution but the large-scale (geostrophic) winds. The temperature profile of De Bilt (station 260, see Figure 1) measured at 0 UTC is used as initial temperature profile in the entire model domain. As initial wind profile, the profile measured with the radio sounding of 12 UTC is used, as the observed wind halfway through a simulated day is on average more representative for the average large-scale conditions during a day than the observed wind at 0 UTC. This is confirmed by the results in the form of the simulated frequency distributions that correspond much more with the observed distributions when the 12 UTC observed winds are used than when the 0 UTC observed winds are used to initialize the model. During every single-day run the large-scale conditions (such as the large-scale wind from the radio sounding) are held constant.

The sea-surface temperature is kept constant during one day. For each individual day it is adjusted according to the measurements made at station 553 (see Figure 1). The sensible heat flux in the surface layer is prescribed during the day, with zero flux at 6 UTC and 18 UTC and a sine-like time dependence in between. The maximum sensible heat flux

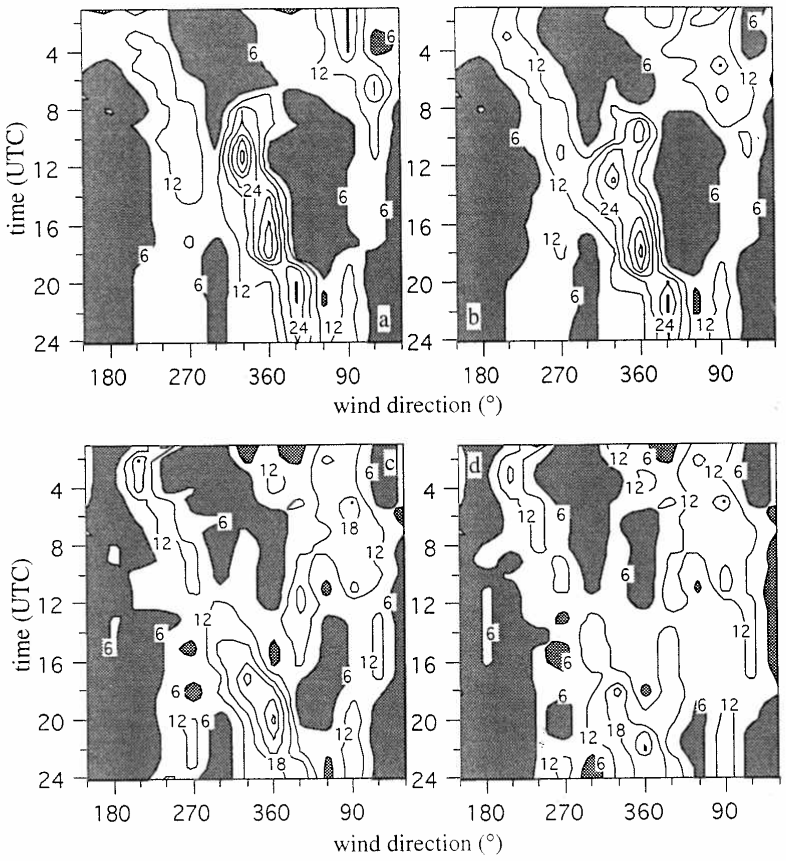

Figure 3: The modeled frequency distributions (%) at the model points at the coast-line (a), 5 km inland (b), 50 km inland (c) and 100 km inland (d) in the period from 1 to 29 May, 1989. The model points represent the observation stations in Figure 2.

varies between H_{max} for sunny days (average cloud cover < 2/8) to $0.5*H_{max}$ for cloudy days (average cloud cover > 6/8). In this study we choose a H_{max} of 250 W m^{-2}, as this value corresponds best to the observed values at Cabauw (Fred Bosveld, personal communication). This value of the maximum surface sensible heat flux, which is rather high for the Netherlands was caused by the drying out of the soil (no precipitation) and the large number of sunshine hours. The observed surface sensible heat fluxes at Cabauw are calculated with methods described in Beljaars and Bosveld (1997). To study the sensitivity to this parameter, we also perform simulations with a H_{max} of 150 and 200 W m^{-2}. During the night the surface sensible heat flux over land is parameterized according to Van Ulden and Holtslag (1985). The surface roughness length is 0.05 m and the latitude is 52°N.

4 Model results

Figure 3a to d shows the results of the model runs producing the best match (compare with Figure 2) which are for a day-time maximum sensible heat flux of 250 W m^{-2}. The observed frequency distribution for station 330 compares well with the modeled frequency distribution. The modeled time of onset of the sea breezes at the coast (about 8 UTC) is as observed. The largest difference is that the modeled maximum

frequency between 8 and 12 UTC is found for a direction of 330° whereas the observed maximum frequency has a direction of 0°. The modeled shift to 30° after sunset is as observed.

The modeled frequency distribution for station 210 (Figure 3b) also resembles the observed distribution well. The two separate maxima for the sea breezes from the (South-) West and Northwest are as observed, with the onset of the sea breezes one to two hours too early in the model runs. The convergence of the two maxima in the early afternoon is caused by the different reaction of the sea breeze to large-scale flow from different directions. The sea breeze that develops in a large-scale flow with a Southerly wind component blows from the Southwest initially. During the day and when the southern component of the large-scale flow is weak enough, this sea breeze veers to the Northwest or North, due to the geostrophic adjustment process. When the large-scale wind has a Northerly component, the sea breeze will come from a Northwesterly direction initially. This is almost parallel to the geostrophic sea breeze direction, so this sea breeze veers only slightly to the North after the onset of the sea breeze. Therefore, the two maxima in the wind direction frequency distribution will converge during the afternoon and evening. The turning of the wind direction to the North in the model late in the afternoon, and further to 30° in the early evening together with the timing of the maximum frequencies is as observed.

Further inland, at station 260 (Figure 3c), the model results also resemble the observations. In the model results as well as in the observations, a maximum frequency can be found for a direction of 330° at 17 UTC. This maximum is caused by the onset of sea breezes. After sunset, the maximum frequency shifts to 30°.

The most important feature for station 375 is the observed maximum frequency for a direction of 0° at 21 to 22 UTC. In the model results (Figure 3d) this high frequency can also be detected around 22 UTC. The model results also show the broad maximum between 30° and 90° during the night and the slow shift in high frequencies from 210° to 270° during the morning and afternoon.

For a lower maximum sensible heat flux, the frequency distributions near the coast are similar to the model results presented here. However, far inland the differences become larger. The largest difference is the much lower maximum frequency of Northerly winds far inland in the evening, which is caused by the weaker and less far inland penetrating sea breezes.

The relatively high frequencies of the Northerly directions in the model as well as in the observations show that sea breezes originating near the West coast can penetrate more than 100 km inland at 52° North. The high frequency of Northerly winds around 22 UTC is probably caused by the acceleration of the sea-breeze front during the evening, because in the model runs there is no evidence of a gravity-inertia wave that travels inland and originates near the sea-breeze front. During the afternoon the sea breeze penetrates with an average speed of about 7 km h^{-1} (from station 210 to station 260 in 7 hours) while during the evening inland penetration takes place at a speed of about 12 km h^{-1} (from station 260 to 375 in 4 hours).

This acceleration during the evening is well known from the literature (e.g. Simpson et al., 1977; Physick, 1980; Sha et al., 1991). Simpson et al. (1977) and Physick (1980) explain the acceleration of the inland penetration of the sea breeze through the decreasing sensible heat flux over land in the afternoon. This leads to less adjustment (warming) of the relatively cool air that is transported over land by the sea breeze, causing an increase in the temperature difference between the air ahead of the sea-breeze front and behind it. This enhances the pressure gradient over the sea-breeze front, leading to stronger accelerations and an increased inland penetration of the sea-breeze front. According to Sha et al. (1991), the difference in penetration speed between the afternoon and evening is caused by the friction at the top of the sea-breeze layer, which is much larger during the afternoon. The larger friction is caused by the occurrence of Kelvin-Helmholtz instability that increases the turbulent mixing.

The observations of station 348 (see Van Delden, 1993) are not used in this study, because they contain a feature that cannot be explained by sea breezes originating near the West coast nor calculated with the 2-D model. The wind-direction frequency distribution at this station shows an increase in Northerly winds as early as 13 UTC, while at station 210, the sea breezes set in around 11 UTC. If the high frequency of Northerly winds at station 348 were caused by sea breezes, the sea-breeze front would travel inland with a speed of about 20 km h^{-1}, as stations 210 and 348 lie about 40 km apart. From simulations and observations it is clear that the average inland penetration speed of the sea-breeze front is 5 to 10 km h^{-1} at the most late in the morning and in the early afternoon. Therefore, it is highly unlikely that the high frequency of Northerly winds at station 348 is caused by sea breezes originating near the West

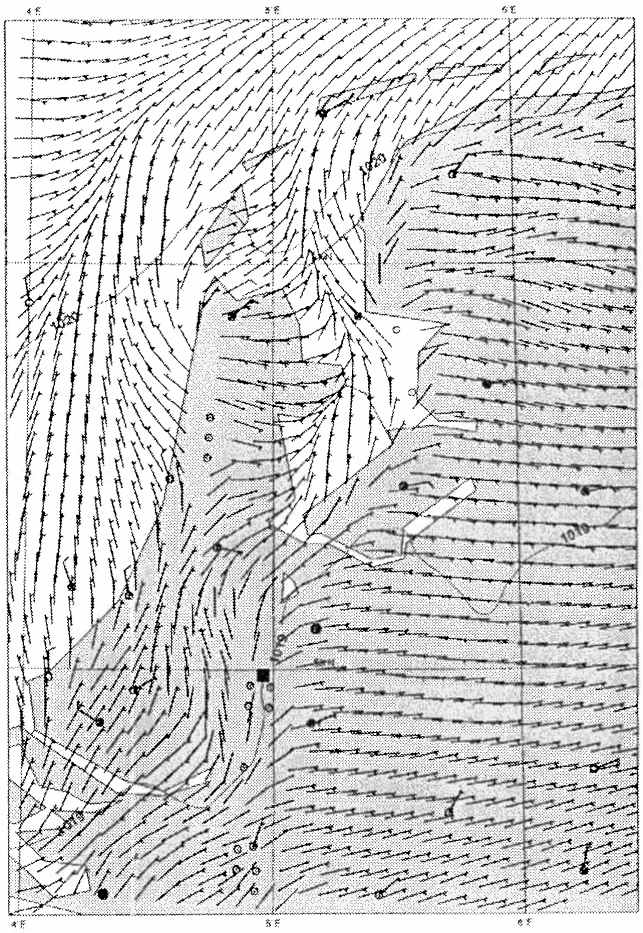

Figure 4: Horizontal wind field and surface-pressure distribution over the Netherlands at 15 UTC on 29 July, 1995, as calculated with the doubly-nested version of VHiRLAM with semi-lagrangian advection. Cabauw lies at 51°58′ N and 4°56′ E indicated by a black square (from De Bruijn, 1997).

coast. An explanation of this phenomenon may be the lake breezes that develop around Lake-IJssel. Experiments with a high-resolution limited area model (VHiRLAM, from De Bruijn, 1997, see Figure 4) show that Lake-IJssel can channel the lake breezes into the western part of the Netherlands, causing a Northerly wind. Station 348 lies near the eastern edge of the area that is influenced, while stations 260 and 265 lie east of the area that is influenced. Therefore the high frequency at station 348 is caused by the lake breezes that cannot be simulated with the 2-dimensional model.

5 Factors Affecting the Inland Penetration

Next we investigate the factors that influence the inland penetration of the sea breeze by performing a

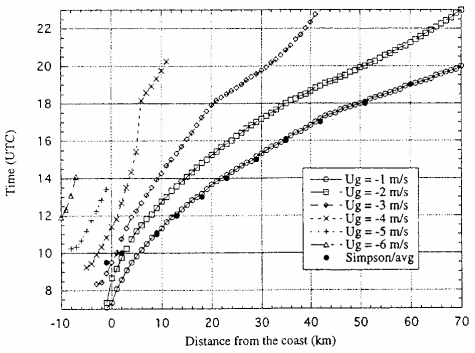

Figure 5: The inland penetration of the sea breeze as a function of the large-scale flow for a maximum day-time sensible heat flux of 200 W m^{-2}. Also plotted is the average inland penetration of the sea breeze in England as found by Simpson et al. (1977, black dots).

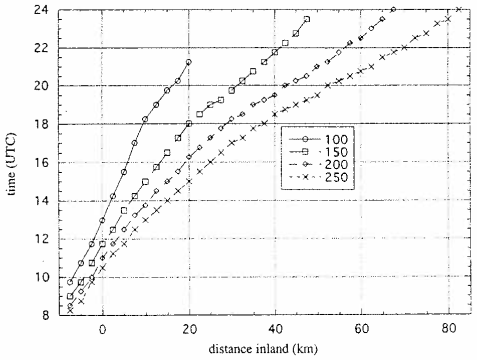

Figure 6: The inland penetration of the sea breeze as a function of the maximum sensible heat flux over land for an opposing large-scale flow of 2 m s^{-2}.

number of sensitivity experiments with the model. We investigate the influence of the large-scale wind opposing the sea breeze, the magnitude of the differential heating, the roughness length of the land surface, the depth of the initial boundary layer and the influence of the higher surface sensible heat flux near the coast due to the advection of cool and moist air over the hot land. The latter effect was also investigated by Arritt (1993).

To demonstrate the inland penetration of the sea-breeze front, we perform six runs with identical initial conditions apart from the large-scale opposing flow. We use the radiosounding of a typical summer day as initial temperature profile (a night-time inversion near the surface, weakly stable or neutral profile up to an inversion at a height of about 1500 m) and a maximum surface sensible heat flux of 200 W m^{-2}. The horizontal grid-point distance is 1000 m.

The results show that sea breezes can reach the Dutch coast for large-scale opposing flows (= U_g) as strong as 5 m s^{-1} (see Figure 5). When the opposing flow is stronger, sea breezes still develop but do not reach the coast. It is also clear that sea breezes develop later and further out to sea with increasing opposing flow.

In the initial stage of development of the sea breeze, the sea-breeze front approaches the coast quite rapidly. However, when the sea breeze travels over land, the propagation speed of the front decreases (e.g. see the case for $U_g = -4$ m s^{-1}). During the afternoon the inland penetration speed remains almost constant, varying from less than 1 km h^{-1} for $U_g = -4$ m s^{-1} to about 5 km h^{-1} for $U_g = -1$ m s^{-1}. Late in the afternoon, Richardson numbers above the sea-breeze layer start to rise. The reduced turbulence at the top of the sea-breeze layer combined with a weaker opposing flow near the surface and a larger temperature difference near the sea-breeze front cause the sea-breeze front to accelerate. After 18 UTC the inland penetration becomes nearly constant in time, varying from about 3 km h^{-1} for $U_g = -4$ m s^{-1} to 11 km h^{-1} for $U_g = -1$ m s^{-1}.

Due to this acceleration (observed by Simpson et al., 1977; simulated by Physick, 1980) the sea breeze can travel far inland, especially in the evening. Therefore it is not surprising that the frequency distribution of station 375 shows a maximum around 21 UTC. What is surprising, however, is the magnitude of the maximum frequency. Simpson et al. found that only 6 of 76 (less than 10%) of the sea breezes that passed Lasham (±43 km inland) also reached Oxford, which lies 105 km inland. As already shown in section 2, deep inland penetrating sea breezes occurred on about 60% of the days with sea breezes at the West coast. This high frequency of deep inland penetrating sea breezes is probably caused by the large number of days in this month with a large-scale flow that was weak or almost parallel to the coast, combined with the relatively large forcing resulting in strong sea breezes.

The average time of onset of the sea breezes in the study of Simpson et al. (1977) is also plotted in Figure 5. The average inland penetration for the 76 cases of sea breeze reaching at least 40 km inland compares well with the inland penetration found with the model

for a U_g of -1 m s^{-1}. This is not surprising because, according to the model, sea breezes can just reach this far inland for an opposing flow of 3 m s^{-1}. For stronger opposing flow the inland penetration is limited to 10 km or less. The average large-scale winds in the cases with sea breezes reaching 40 km or more inland will therefore be close to -1 m s^{-1}.

In Figure 6 the results of a sensitivity experiment with different prescribed sensible heat fluxes are plotted. In this experiment the maximum sensible heat flux ranges from 100 to 250 W m^{-2}, the grid-point distance is 2500 m, the large-scale flow is -2 m s^{-1} and the initial depth of the boundary layer is 1000 m. The maximum inland penetration clearly increases with increasing differential heating. When the sensible heat flux over land is 100 W m^{-2}, the maximum inland penetration is only 20 km. The maximum distance of inland penetration still has not been reached at 24 UTC when the maximum sensible heat flux is 250 W m^{-2}. The inland penetration distance is not a linear function of the maximum sensible heat flux. From this experiment we can conclude that the magnitude of the differential heating is important for the inland penetration of the sea breeze.

Additional experiments show that the sensitivity of the inland penetration to changes in the roughness length over land, the initial depth of the boundary layer and the calculation of the sensible heat flux with the soil temperature from a soil module is negligible.

6 Scaling the Inland Penetration

In the previous section we show two figures where the inland penetration is a function of the large-scale flow (Figure 5) and where the inland penetration is a function of the forcing, i.e. the surface sensible heat flux (Figure 6). In this section we try to find a scaling for the inland penetration of the sea breeze.

Steyn (1998) finds a scaling for the average strength of the cross-coast sea-breeze component by fitting observations to combinations of non-dimensional parameter groups that govern the sea breeze. In Tijm and Holtslag (1999), this expression is simplified and generalized with a latitude dependence by fitting the equation to model output at different latitudes. This results in:

$$U_m = \gamma_1 \left(1 + \gamma_2 cos^3\phi\right) (NT_h)^{-1/4} \left[\frac{g}{\Theta_0} \int_0^{T_h} \Delta(\overline{w'\Theta'})_0 dt\right]^{1/2}, \qquad (6.1)$$

where U_m is the maximum cross-coast component of the sea breeze that develops during the day, ϕ is the latitude, N is the Brunt-Väisälä frequency measured above the sea-breeze layer, where the temperature profile is always stable, g is the gravity acceleration, Θ_0 is the potential temperature, $\int_0^{T_h} \Delta(\overline{w'\Theta'})_0 dt$ is the differential surface sensible heat flux between the land and the sea, T_h is the period with a positive differential heating (where $(\overline{w'\Theta'})_0$ over land is larger than over sea) and γ_1 and γ_2 are two coefficients, equal to 1.7 and 0.5, respectively. Equation 6.1 shows that the maximum cross-coast sea-breeze component is mostly determined by $\sqrt{\Delta(\overline{w'\Theta'})_0}$, the heating period and the latitude. For example, this equation results in a U_m of about 7 m s^{-1} if we use an average differential heating of 127 W m^{-2}, a heating period of 12 hours, $N \sim 0.01$ s^{-1} and Θ_0 is 300 K at 0° of latitude.

With the scaling of the penetration distance of the sea breeze we want to find a characteristic curve of the inland penetration. This can be achieved by dividing the actual inland penetration distance (x) by a linear combination of the large-scale opposing wind (U_g) and the maximum cross-coast sea-breeze strength (U_m, from equation 6.1). This results in an inland penetration time scale τ_s:

$$\tau_s = \frac{x}{\mu_m U_m - \mu_g U_g}, \qquad (6.2)$$

where μ_m and μ_g are dimensionless coefficients.

Figure 7 clearly shows the succes of Eq. 6.2 in predicting the inland penetration. All curves of the inland penetration lie approximately on one characteristic line, except when the large-scale flow becomes too strong. This is the case when U_g is -4 m s^{-1}. Note that the data of Simpson et al. (1977) also lie on this characteristic line. The coefficients μ_m and μ_g are 0.7 and 0.8, respectively, which are determined from least-square fitting. Apparently, U_m and U_g have a characteristic ratio of 0.875 over land with the characteristics of the Netherlands. The results deteriorate considerably if we take another ratio for these two coefficients. The magnitude of this ratio is probably related to two effects. First, the average cross-coast component in the sea-breeze layer is about 60 to 70% of the maximum cross-coast component. Second, this average cross-coast sea breeze is opposed by a large-scale wind that does not have the strength of the geostrophic wind, because the wind is slowed down by the friction with the surface. Turbulence within the boundary layer spreads the influence of the surface friction through the entire boundary layer,

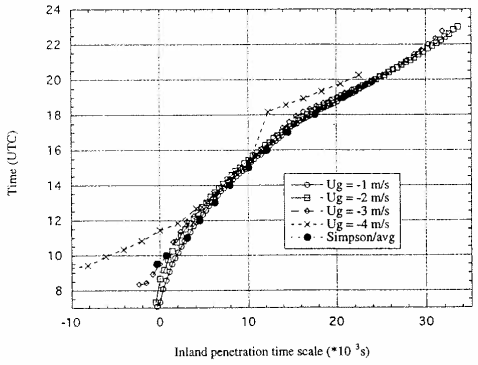

Figure 7: The inland penetration time scale of the sea breeze, forced by a maximum sensible heat flux of 200 W m^{-2}, at 52°N for large-scale opposing winds ranging from -1 to -4 m s^{-1}. The observations of Simpson et al. (1977) are shown also. The coefficients μ_m and μ_g are 0.7 and 0.8, respectively.

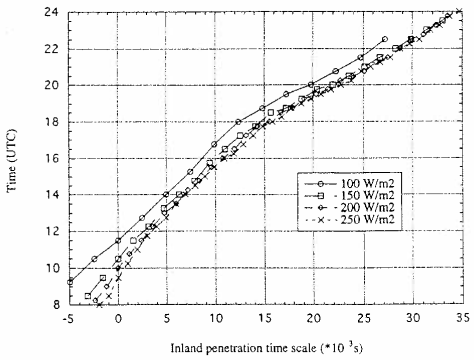

Figure 8: The inland penetration time scale of the sea breeze, opposed by a geostrophic wind of -2 m s^{-1}, at 52°N for maximum differential heating ranging from 100 to 250 W m^{-2}. The coefficients μ_m and μ_g are the same as in Figure 7.

causing the large-scale wind to be about 75 to 80% of the geostrophic wind in the bulk of the boundary-layer. Therefore, the sea breeze is not opposed by the geostrophic wind, but only by a fraction of this wind.

The scaling of Eq. 6.2 is confirmed when we apply it to the inland penetration as a function of the forcing through the sensible heat flux. Figure 8 again shows that the model results for the different heat fluxes lie approximately on a single line, except for the heat flux of 100 W m^{-2}, where the maximum cross-coast sea-breeze component comes too close to the strength of the opposing large-scale flow. Note that the line that is found in this second experiment is not exactly the same as in the first experiment. This is probably caused by the different resolutions and associated diffusion coefficients that are used in the two experiments.

These results show that we now can predict (to some extent) the time of arrival of the sea-breeze front at a certain place if we have estimates of the day-time surface sensible heat flux over land (for the calculation of U_m) and the large-scale wind.

7 Analysis of the Daily Cycle of the Surface Pressure

To investigate if the daily cycle of the surface pressure shows a pressure anomaly that resembles a gravity-inertia wave as found by Van Delden (1993) and that is connected to the high frequency of Northerly winds at inland stations in the evening, only 14 of the 29 days available can be used because of gaps in the surface-pressure data of the stations at sea. The characteristics of these remaining 14 days are described in Van Delden (1993). The average daily cycle of the surface pressure (see Figure 9) shows that the pressure signal is dominated by the atmospheric tide. A second conclusion from this figure is that the surface pressure increases more over sea than over land, with the largest increase farthest out at sea. This is probably caused by the formation of the thermal low over the European continent.

In order to compare the pressure cycles due to sea-breeze effects at individual stations we must remove the average tidal signal. This can be achieved by subtracting the average daily cycle of the surface pressure at all stations from the individual daily cycles. This operation, together with the subtraction of the average daily pressure perturbation that is performed earlier to correct for systematic measuring errors, can introduce an unwanted effect in the final result for the stations that are influenced by the sea breeze. This is illustrated in Figure 10 where three fictitious daily cycles of the surface pressure perturbation are plotted, one of a station far out at sea, one near the coast that is influenced by the sea breeze and one far from the coast over land. These fictitious pressure-perturbation cycles are already corrected for the semi-diurnal atmospheric tide and only show the pressure perturbations caused by diabatic heating and temperature advection. Subtracting the daily average from the daily cycle does not change anything at the stations far out at sea and far from

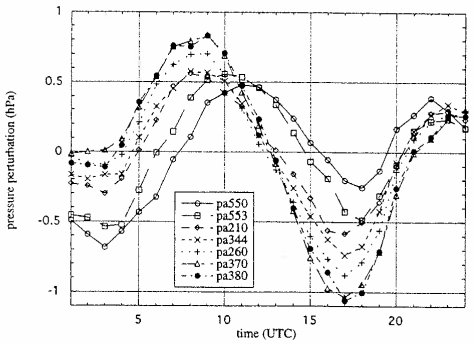

Figure 9: Average daily cycle of the surface-pressure perturbation from the hourly mean surface pressure at 7 stations for the 14 days in the study by Van Delden (1993).

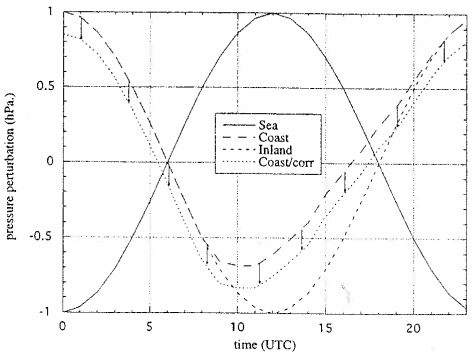

Figure 10: The effect of the subtraction of the daily average pressure perturbation from the daily cycle of the pressure perturbation, that already is corrected for the atmospheric tides, at a station influenced by sea breezes. The effect of the subtraction is indicated by the arrows.

the coast over land, that are not influenced by sea breezes. At these stations, the daily average of the pressure perturbation is zero. At the station near the coast, the sea breeze has the effect of increasing the surface pressure late in the morning and in the afternoon through the advection of cool sea air, an effect that is superimposed upon a daily cycle of the pressure perturbation that is identical to the surface pressure perturbation cycle at the station far inland. Therefore, the daily average pressure perturbation will be positive. The subtraction of this positive daily average has the effect of lowering the curve of the daily cycle (indicated by the arrows in Figure 10). This causes the pressure perturbation to be lower near the coast during the night and morning, after which this area of relative low pressure will move inland to locations that experience less influence of the sea breeze or which experience this influence later in the afternoon. This is exactly what is found in the study by Van Delden (1993) that we have followed so far.

If we plot the pressure perturbation *tendency* instead of the pressure perturbation, we can evade the artifact of the analysis by Van Delden (1993). Figure 11 clearly shows that the largest relative pressure changes occur farthest from the coast. These changes are largest over sea due to the larger number of land-based stations that are used in the averaging procedure. In Figure 11 there is no evidence of a low pressure anomaly travelling inland, as there is no area of increased negative tendency that travels inland. The suggestion that the high frequency of Northerly winds far inland is caused by a gravity-inertia-like wave, originating at the sea-breeze front,

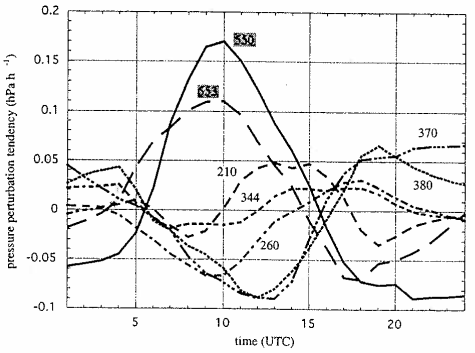

Figure 11: Average daily cycle of the pressure perturbation tendency at 7 stations for the 14 days in the study by Van Delden (1993). The shaded labels indicate the stations at sea.

cannot be substantiated by the current analysis. The simulations and new pressure analysis show that the high frequency of Northerly winds is caused by an anomalously high percentage of deep penetrating sea breezes, due to the large number of days with a weak or along-shore large-scale flow.

8 Conclusions

In this study we have used a two-dimensional numerical model to reproduce the observed high frequency of Northerly winds (parallel to the coast) in the evening at a station in the Netherlands that lies as

far as 100 km inland. The observed frequency distributions of the wind direction of May, 1989, are successfully reproduced with the numerical model.

From an improved method of analysis of the average daily pressure cycles it must be concluded that there was no negative pressure anomaly connected to the high frequency of Northerly wind far inland. A detailed investigation of the days with Northerly winds far inland in the evening also showed that the Northerly wind usually was not preceded by a Southerly wind. Therefore, the explanation of Van Delden (1993) that this high frequency was caused by gravity-inertia waves cannot be confirmed. The high frequency of Northerly winds far inland in the evening is caused by sea breezes that penetrate very deep inland due to a large number of days with a weak or along-shore large-scale flow.

The sea breezes can travel this deep inland because the rate of inland penetration increases during the afternoon and evening. This acceleration is caused probably by a combination of decreasing friction at the top of the sea-breeze layer, weaker opposing flow near the surface due to increased stability and larger temperature and pressure gradients near the sea-breeze front. The larger temperature gradients are caused by the decreasing adjustment of the sea air advected over land by the sea breeze in the afternoon, due to the decreasing sensible heat flux.

The most important factors that influence the distance of the inland penetration are the opposing large-scale flow and the magnitude of the differential heating driving the sea breeze. Factors that have very little influence on the inland penetration rate are the surface roughness, the initial depth of the boundary layer and the effect of the increasing sensible heat flux behind the sea-breeze front due to the advection of cool and moist air over a relatively warm land surface. The model results for an opposing flow of -1 m s^{-1} and a maximum sensible heat flux of 200 W m^{-2} compare well with the average inland penetration speed of sea breezes reaching at least 40 km inland in England (Simpson et al., 1977). This is particularly true when the findings are scaled.

The scaling of the inland penetration with a combination of U_m and U_g results in a inland-penetration time scale. All inland penetration curves from the sensitivity experiments converge on one characteristic line, except when the value of U_m lies too close to U_g. From this characteristic line, the inland penetration of the sea breeze can be predicted if U_m (i.e. the daytime surface sensible heat flux over land) and U_g are known.

References

Arritt R.W., 1993: Effects of the large scale flow on characteristic features of the sea breeze. J. Appl. Meteor. **32**, 116–125.

Atkinson B.W., 1981: Meso-scale atmospheric circulations. Academic press, 495pp.

Beljaars A.C.M. and Bosveld F.C., 1997: Cabauw data for the validation of land surface parameterization schemes. J. Climate. **10**, 1172–1193.

De Bruijn E.I.F., 1997: Experiments with horizontal diffusion and advection in a nested fine mesh mesoscale model. IMAU-report V 97-22, Utrecht, 32pp.

Holtslag A.A.M. and Boville B.A., 1993: Local versus non-local boundary-layer diffusion in a global climate model. J. Climate. **6**, 1825–1842.

Physick W.L., 1980: Numerical experiments on the inland penetration of the sea breeze. Q. J. R. Meteorol. Soc. **106**, 735–746.

Sha W., Kawamura T., and Ueda H., 1991: A numerical study on sea/land breezes as a gravity current: Kelvin-Helmholtz billows and inland penetration of the sea-breeze front. J. Atmos. Sci. **48**, 1649–1665.

Simpson J.E., Mansfield D.A., and Milford J.R., 1977: Inland penetration of sea-breeze fronts. Q. J. R. Metorol. Soc. **103**, 47–76.

Steyn D.G., 1998: Scaling the vertical structure of sea breezes. Boundary-Layer Meteorol. **86**, 505–524.

Tijm A.B.C. and Holtslag A.A.M., 1999: Sea-breeze scaling and mesoscale fluxes. In preparation.

Tijm A.B.C., Holtslag A.A.M., and van Delden A.J., 1999: Observations and modelling of the sea breeze with the return current. Mon. Wea. Rev. **127**, 625–640.

Van Delden A.J., 1993: Observational evidence of the wave-like character of the sea breeze effect. Contr. Atmos. Phys. **66**, 63–72.

Van Ulden A.P. and Holtslag A.A.M., 1985: Estimation of atmospheric boundary layer parameters for diffusion applications. J. Climate Appl. Meteor. **24**, 1196–1207.